

MORPHOMETRIC LOCALIZATION OF MANDIBULAR FORAMEN IN A SAMPLE OF ADULT SAUDIAN POPULATION USING CONE-BEAM COMPUTED TOMOGRAPHY

Mohamed Mehanny ^{*,**}, Soad Mansour ^{***}, Atiaf Alzahrani ^{****}, Lama Alquraishi ^{****},
Razeem Alhassoun ^{****} and Rasha H. Al-Serwi ^{*****}

ABSTRACT

The aim of this retrospective study was to analyse the location of the mandibular foramen (MF) in the vertical and horizontal planes by using a cone-beam computed tomography (CBCT) volumetric data set obtained from an adult Saudi population. CBCT data from 57 females and 50 males (mean age, 38 years; range, 20–56 years) were randomly selected from the Oral & Maxillofacial Radiology Division, Faculty of Dentistry, Princess Nourah Bint Abdulrahman University, between 2017 and 2019. CBCT images were acquired using an i-CAT three-dimensional (3D) imaging system. Standardization of the 3D-rendered volume within the three coordinates was performed. All radiographs were interpreted independently by two observers, and there was satisfactory intra- and inter-observer agreement. All measurements (MF/deepest point at the anterior border of the ramus [A], MF/most convex point of the mandibular angle [I], MF/deepest point of the mandibular sigmoid notch, MF/deepest point at the posterior border of the ramus, MF/reference occlusal plane line) were performed on both the right and left rami on a total of 214 CBCT scans. MF/A ($P = 0.001$) and MF/superior vertical height ($P = 0.0082$) were significantly different between age groups, while males and females exhibited significant differences in MF/I ($P = 0.0045$) and MF/superior vertical height ($P = 0.0297$). The study results indicated that the MF is located posteriorly and superiorly and its position is directly correlated with patient age and sex. Therefore, patient age and sex may be used to predict MF location, thereby facilitating the administration of IAN block anaesthesia and orthognathic surgery.

KEYWORDS: Cone Beam Computed Tomography, Mandibular Foramen Location.

* Basic Dental Sciences, College of Dentistry, Princess Nourah Bint Abdulrahman University, Saudi Arabia
** Oral Radiology Department, Faculty of Dentistry, University of Minia, Egypt
*** Oral Radiology Department, Faculty of Dentistry, Cairo University, Egypt
**** Dental Intern, Princess Nourah Bint Abdulrahman University, Saudi Arabia
***** Oral Biology Department, Faculty of Dentistry, Mansoura University, Egypt

INTRODUCTION

The mandibular foramen (MF) is an important anatomical structure located on the ramus of the mandible and is the opening at which the inferior alveolar nerve (IAN) and vessels enter the mandibular canal. The IAN gives off sensory branches to the inferior dental plexus. The nerve exits the mandibular canal through the mental foramen as the mental nerve, which supplies sensory branches to the skin of the chin, and mucosa of the lower lip^[1].

The IAN block is the most commonly used method to achieve anaesthesia during surgical procedures (e.g., tooth extraction, dental implantation) in the mandible^[2]. However, as the anaesthetic is delivered directly above the MF, the effect is often inadequate if the surgeon does not accurately identify the anatomical site of the foramen or if the foramen has been dislocated^[2]. In addition, orthognathic surgery for maxillofacial deformities and aesthetic indications may result in complications (e.g., damage to the IAN and local blood vessels), unless the foramen is precisely located^[3]. Therefore, recently sagittal split ramus osteotomy became frequent surgical treatment for the rectification of dentofacial deformities due to its advantages, such as an internal approach, easy internal fixation and early jaw function^[4-5].

Determining the accurate anatomical location of the MF and mandibular lingula (ML) is important to achieve a clear fracture line on the ramus and prevent IAN damage^[4]. The ML has been labelled as an essential surgical landmark for horizontal osteotomy in orthognathic surgery, as the horizontal line is situated close to the ML and IAN^[4-6]. The precise determination of its location is also critical for the surgical management of mandibular trauma, tumour removal, as well as mandibular and temporomandibular joint reconstruction^[7].

Nevertheless, the estimated failure rate of the IAN block has been stated to range between 10% and 39%^[8, 9]. The most common cause of

block failure has been reported to be the incorrect placement of the hypodermic needle tip, such that it is too far away from the MF^[10]. This suggests that the location of the IAN may vary within the patient population. This variation in location has been reported by numerous studies, and several alternative anaesthesia techniques, such as the Gow-Gates and Vazirani—Akinosi injections, have been proposed to manage this issue^[11-12]. However, none of these alternative reported techniques reported have been able to consistently provide has resulted in an increased rate of successful rate by delivering consistent IAN anaesthesia. Furthermore, the majority of prior most studies have do not reported the indicate a range of variation in MF location^[13].

If anaesthesia is not achieved with the first attempt of the IAN block, a second injection would be necessary, due to the assumption that the needle was placed inaccurately. However, this is often a blind attempt, which usually uses the same intraoral landmarks used to guide the first injection^[14, 15]. Therefore, proper evaluation of anatomical landmarks, such as the ML and MF, is the key to achieving adequate IAN anaesthesia in routine dental practice^[16].

The implementation of cone-beam computed tomography (CBCT) in dentistry field has rapidly grown recently. CBCT has several advantages over conventional medical computed tomography, such as a lower radiation dose, shorter radiation exposure time and higher resolution ratio. It has been mentioned that the radiation dose of CBCT is only 25% of that of a panoramic radiograph and 1.6–2.5% of the dose of a conventional medical CT image^[17, 18]. One of the most remarkable advantages of CBCT is its high resolution, as it provides a voxel size as small as 0.125 mm; this facilitates the generation of highly accurate three-dimensional (3D) reconstructions^[19-20].

Conventional radiographic techniques are associated with distortion and magnification of the imaged anatomical structures^[21-23]. These imaging

flaws range from 3.4% for periapical radiographs to >14% for panoramic radiographs; therefore, conventional radiographs are insufficiently accurate for measuring angulation and height above the mandibular occlusal plane^[21]. Recent studies^[23–24] evaluating the accuracy of digital measurements obtained via CBCT imaging software reported an error range between 0.07 and 0.27 mm when compared with known standardised measurements. These studies also reported a distortion of <1.8% in the images, as well as a high sensitivity for the accurate identification of anatomical structures^[21, 22–24].

The objectives of this retrospective study were to assess MF location with CBCT and identify its range of normal variability with specific landmarks, as well as evaluate the association between MF location and both patient age and sex in Saudi population. The overarching aim was to provide an accurate guide for IAN block administration using CBCT, thereby increasing the safety and effectiveness of anaesthesia and surgical procedures.

MATERIALS AND METHODS

The ethics committee at the College of Dentistry Research Centre, Princess Nourah Bint Abdulrahman University (PNU), Saudi Arabia, approved the study protocol (institutional review board number: 19-0282) and provided ethical guidelines. This retrospective study included 107 Saudi patients (214 CBCT images) who were collected from the Oral and Maxillofacial Radiology Division, Faculty of Dentistry, PNU, between 2017 and 2019. The samples were experimental design and calculated depending on anticipated effect size, desired statistical power level, number of predictors, and probability level. All the patients had been referred for CBCT scans with large field of view (FOVs). CBCT images were acquired using an i-CAT 3D imaging system (Imaging Science International, USA 2008). The imaging parameters were set as follows: 12mA

and 90 kVp with an FOV of 80 x 100 mm. Using the CBCT data, the 3D models of the selected cases were rendered using the Planmeca Romexis® Viewer 6.0 software program, with a voxel size of 0.2 mm, and slice thickness of 0.2 mm. All scans were viewed on an LCD Dell monitor with a 24-inch screen size and 1920 x 1080 high-definition screen resolution.

Inclusion and exclusion criteria

The inclusion criteria comprised the following: (1) CBCT data of the mandibular ramus obtained from adult patients (aged >18 years); and (2) presence of premolars and molars for the identification of the occlusal plane. Patients with mandibular edentulism or a history of mandibular pathology or surgery were excluded.

Standardisation of 3D images

Prior to conducting radiographic measurements, the 3D-rendered volume was standardised by the automatic selection of the reference line buttons, such that the 3D images were oriented in the horizontal and vertical planes. According to the horizontal reference line, the occlusal plane was simultaneously oriented parallel and perpendicular to the vertical reference line. Using the software clipping icon, the mandible was clipped from the buccal to the lingual direction to obtain measurements of the MF. Measurements between the anatomical reference points were performed using the Planmeca Romexis® Viewer 6.0 software measuring tool. Standardisation steps were performed by an expert maxillofacial radiology specialist and an adequately calibrated examiner.

CBCT analysis and measurement techniques

Calibration sessions were conducted prior to performing the radiographic measurements; these sessions included practical discussion on mandibular CBCT landmarks by a senior maxillofacial radiologist in the PNU clinics. The examiners performed

the radiographic measurements independently and blindly. The confidence interval (CI) 95% and inter-examiner reliability were then determined. The reliability levels ranged from 90% to 94%.

The calibrated examiners measured the shortest distance (in mm) between the landmarks using a digital ruler. The selected landmarks were as follows (Figure 1):

- 1- “MF” (opening of the MF);
- 2- “ML” (tip of the ML);
- 3- “A” (deepest point at the anterior border of the ramus);
- 4- “P” (deepest point at the posterior border of the ramus);
- 5- “S” (deepest point of the mandibular sigmoid notch);
- 6- “I” (most convex point of the mandibular angle); and
- 7- “O” (reference occlusal plane line connecting the mesiobuccal line angle of the second premolar to the mesiobuccal cusp tip of the second mandibular molar).

The measured distances were reported as the shortest distances from the MF to A, P, S, I and O. In addition, the location of the MF in the horizontal

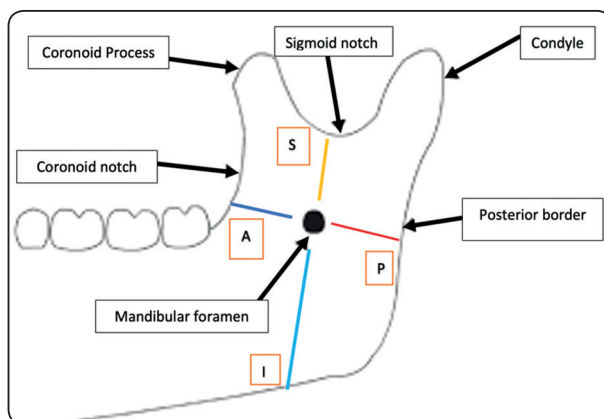


Fig. (1): Photograph showing the anatomical landmarks and reference points.



Fig. (2): 3D rendering reveals the linear measurements of MF location as; MF/S = 15.6mm, MF/I= 26.2 mm, MF/A= 15.1 mm, MF/P= 11.3 mm, AP= 27.3 mm, and SI= 42.7mm.

and vertical planes was calibrated using the following ratios^[19, 25, 26]: A-MF/A-P (MF location in the horizontal plane); and S-MF/S-I (MF location in the vertical plane) (Figure 2). All measurements were performed on both the right and left rami; hence, 107 Saudi patients (214 CBCT scans) were analysed.

Statistical analysis

Data were statistically analysed to determine the location of the MF in the antero-posterior and vertical planes. In addition, the location of the MF was determined with reference to the occlusal plane. The distribution of numerical data was assessed for normality using the Kolmogorov–Smirnov and Shapiro–Wilk tests. All data showed a normal (parametric) distribution. Data are presented as mean, standard deviation (SD) and 95% CI values. For parametric data, a repeated measures analysis of variance (ANOVA) test was used to compare radiographic measurements between males and females, as well as between patients in their early and late adulthood. Bonferroni’s post-hoc test was used for pairwise comparisons when the ANOVA test was significant. The significance level was set at $P \leq 0.05$. Statistical analysis was performed using IBM SPSS Statistics for Windows, version 23.0 (Armonk, NY: IBM Corp.).

RESULTS

A total of Saudi 107 patients; (214 MF) (57 women [53.3%]; 50 men [46.7%]) with the mean ± standard deviation values for age were 35.9 ± 11.1 years were assessed. The majority of patients (59.8%) were in their early adulthood (20–39 years old); 40.2% of the patients were in their late adulthood (40–56 years old).

Comparisons of mean radiographic measure-

ments of the left and right mandibular rami between males and females indicated that females had significantly lower mean values for MF/I ($P = 0.001$, effect size = 0.098), L/O ($P = 0.010$, effect size = 0.061) and SI ($P = 0.004$, effect size = 0.075) (Table 1). In terms of the right side, females exhibited significantly lower mean values for MF/I, MF/O, L/O and SI compared to males. In terms of the left side, mean values for MF/I and SI were significantly lower in females (Table 1).

TABLE (1) Descriptive statistics and results of the analysis of variance test for comparison of different measurements between males and females.

Side	Measurement	(57 = Females (n		(50 = Males (n		P-value	Effect size (Partial Eta Squared
		Mean	SD	Mean	SD		
Right side	MF/A	14.19	2.45	15.04	2.42	0.073	0.03
	MF/P	12.41	2.52	12.42	2.22	0.978	0.00001
	MF/S	15.38	3.12	15.23	2.68	0.791	0.001
	MF/I	23.96	3.35	26.43	5.53	*0.006	0.071
	MF/O	3.01	2.16	4.03	2.87	*0.038	0.04
	L/O	6.2	2.19	7.6	2.93	*0.006	0.071
	AP	26.96	4.81	27.61	3.98	0.457	0.005
	SI	37.92	7.18	41.4	6.76	*0.012	0.059
Left side	MF/A	14.2	2.46	15.72	7.22	0.138	0.021
	MF/P	12.98	2.66	13.66	2.71	0.192	0.016
	MF/S	15.43	2.78	15.78	3.05	0.533	0.004
	MF/I	23.32	3.68	26.16	4.23	*0.001>	0.117
	MF/O	2.42	2.27	2.86	2.07	0.305	0.01
	L/O	5.88	2.22	6.45	1.75	0.143	0.02
	AP	27.2	4.19	27.88	3.98	0.393	0.007
	SI	38.75	5.84	42.25	6.33	*0.004	0.078
Mean of the two sides	MF/A	14.21	2.22	15.41	4.14	0.060	0.033
	MF/P	12.73	2.45	13.06	2.28	0.477	0.005
	MF/S	15.44	2.78	15.55	2.61	0.832	0.0004
	MF/I	23.66	3.39	26.32	4.71	*0.001	0.098
	MF/O	2.73	2.09	3.48	1.92	0.057	0.034
	L/O	6.05	2.06	7.05	1.88	*0.010	0.061
	AP	27.11	4.21	27.75	3.86	0.412	0.006
	SI	38.36	5.95	41.84	6.4	*0.004	0.075

Comparisons of mean radiographic measurements of the left and right sides between age groups indicated that patients in their early adulthood had significantly lower mean values for MF/A ($P = 0.001$, effect size = 0.1), AP ($P = 0.027$, effect size = 0.046) and SI ($P = 0.050$, effect size = 0.036) compared to patients in their late adulthood (Table 2). In

terms of measurements on the right side, patients in their early adulthood had a significantly lower mean SI compared to patients in their late adulthood. In terms of the left side, patients in their early adulthood had a significantly lower mean MF/A and AP (Table 2).

Table 2. Descriptive statistics and results of the repeated measures analysis of variance test for the comparison of different measurements between the early and middle adulthood age categories.

Side	Measurement	Early adulthood (n = 64)		Late adulthood (n = 43)		P-value	Effect size (Partial Eta Squared)
		Mean	SD	Mean	SD		
Right side	MF/A	14.33	1.98	14.96	3.03	0.194	0.016
	MF/P	12.17	2.33	12.77	2.41	0.198	0.016
	MF/S	15.3	2.6	15.33	3.35	0.958	0.00003
	MF/I	24.53	4.29	25.98	5.05	0.113	0.024
	MF/O	3.18	2.4	3.94	2.74	0.129	0.022
	L/O	6.59	2.38	7.24	2.98	0.212	0.015
	AP	26.86	4.22	27.86	4.72	0.255	0.012
	SI	38.07	7.25	41.76	6.53	0.008*	0.064
Left side	MF/A	13.47	2.47	17.06	7.29	<0.001*	0.113
	MF/P	12.9	2.58	13.9	2.77	0.061	0.033
	MF/S	15.69	2.79	15.46	3.09	0.699	0.001
	MF/I	24.11	4.31	25.44	3.88	0.107	0.025
	MF/O	2.78	2.24	2.4	2.09	0.377	0.007
	L/O	6.4	1.91	5.77	2.15	0.115	0.024
	AP	26.51	3.51	29.02	4.46	0.002*	0.091
	SI	39.9	6.28	41.11	6.33	0.329	0.009
Mean of the two sides	MF/A	13.92	1.98	16.03	4.34	0.001*	0.1
	MF/P	12.55	2.25	13.37	2.49	0.080	0.029
	MF/S	15.53	2.48	15.43	2.99	0.850	0.0003
	MF/I	24.34	4.17	25.75	4.3	0.095	0.026
	MF/O	3	2.2	3.2	1.77	0.630	0.002
	L/O	6.52	2.03	6.52	2.06	0.998	0.000001
	AP	26.7	3.62	28.46	4.44	0.027*	0.046
	SI	39	6.27	41.46	6.33	0.050*	0.036

DISCUSSION

The MF is a significant anatomical structure located on the ramus of the mandible^[1,27]. The accurate determination of its anatomical position is integral to achieving optimal IAN anaesthesia, as well as preventing intraoperative complications, such as bleeding and permanent neurological damage due to neurovascular bundle transection^[26,28].

CBCT provides surgeons with numerous advantages over conventional tomography and plain films. Therefore, CBCT is considered the radiographic technique of choice for the accurate identification of MF location^[29,30]. Furthermore, the landmarks used with CBCT have the advantages of simplicity, accessibility and the capability to be easily transposed to the patient. As such, they are more likely to be used by oral and maxillofacial surgeons to guide IAN block administration and plan ramus osteotomy lines, which are approaching from the external surface.

The location of the MF may be affected by individual, racial, ethnic and age-related variations^[15, 26, 28,30,31]. The present study evaluated MF location in Saudi population 50 (46.7 %) men and 57 (53.3%) women (mean age, 38 years; range, 20–56 years) via mandibular CBCT 3D-reconstructed radiographs. CBCT radiographs were obtained over a period of 3 years, and the sample size in this study was comparable to that of previous studies utilising similar designs and methodologies^[28,29,32,33].

The findings of this study indicate that in Saudi population the position of the MF is highly bilaterally symmetrical. In terms of sex differences, the MF to inferior mandibular angle distances in males were significantly higher than those in females. This result is supported by the findings of previous studies that utilised CBCT and conventional radiographs^[25,34,35]. Nevertheless, current evidence indicates that observed sexual dimorphisms in bone size and thickness can be attributed to a combination of environmental and genetic factors^[36,37].

In terms of differences in MF location according to age, the present study found that patients in their early adulthood had significantly lower mean measurements for MF/A, AP and SI compared to those in their late adulthood. These findings are in concordance with the fact that the position of the MF and other landmarks are not stationary and are affected by growth and remodelling that occurs with advancing age. The ramus develops by a combination of resorption and deposition on the anterior and posterior regions of the ramus, respectively. These processes extend up to the coronoid process, involving the mandibular notch. The attachment of the elevator muscles to the ramus determines the final size and proportion of the mandibular ramus. The remodelling process continues until the bone reaches adult size, providing the necessary space for permanent molar teeth. In old age, the deposition and resorption processes are imbalanced, resulting in a decreased ramus size; this causes the MF position to shift in the anterior and superior directions^[38-40]. This may explain the posterior shift of the MF in the present study, from a MF/A of 13.9 and 16.3 in early and middle adulthood and the mean (MF-A)/AP was 56.42. and (MF-S)/S-I was 39.08 respectively. However, in the vertical dimension, the MF was located superiorly, with a mean (MF-S)/S-I of 39.08 in late adulthood. This was in agreement with the results of the CBCT study conducted by Altunsoy (2014), who concluded that the MF continued to move in a more superior direction^[25].

CONCLUSIONS

The results of this study indicated that the MF is located posteriorly and superiorly on the ramus. Furthermore, MF position is directly correlated with sex and age group. Therefore, sex and age group may be particularly useful for the prediction of MF location, thereby facilitating the administration of IAN block anaesthesia and orthognathic surgery. Further clinical studies are required to validate the parameters used in this study.

Conflicts of Interest

The authors declare that there is no conflict of interest regarding the publication of this paper.

REFERENCES

- Kaffe I, Ardekian L, Gelerenter I, Taicher S. Location of the mandibular foramen in panoramic radiographs. *Oral Surg Oral Med Oral Pathol*. 1994; 78(5):662–669.
- Hetson G, Share J, Frommer J, Kronman JH. Statistical evaluation of the position of the mandibular foramen. *Oral Surg Oral Med Oral Pathol*. 1988; 65(1):32–4.
- Yoshida T, Nagamine T, Kobayashi T, Michimi N, Nakajima T, Sasakura H et al. Impairment of the inferior alveolar nerve after sagittal split osteotomy. *J Craniomaxillofac Surg*. 1989; 17(6):271–277.
- Monnazzi MS, Passeri LA, Gabrielli MF, Bolini PD, de Carvalho WR, da Costa Machado H. Anatomic study of the mandibular foramen, lingula and antilingula in dry mandibles, and its statistical relationship between the true lingula and the antilingula. *Int J Oral Maxillofac Surg*. 2012; 41(1):74–78.
- Noletto JW, Marchiori E, Da Silveira HM. Evaluation of mandibular ramus morphology using computed tomography in patients with mandibular prognathism and retrognathia: relevance to the sagittal split ramus osteotomy. *J Oral Maxillofac Surg*. 2010; 68(8):1788–1794.
- Smith BR, Rajchel JL, Waite DE, Read L. Mandibular ramus anatomy as it relates to the medial osteotomy of the sagittal split ramus osteotomy. *J Oral Maxillofac Surg*. 1991; 49(2):112–116.
- Kositbowornchai S, Siritapetawee M, Damrongrungruang T, Khongkankong W, Chatrchaiwiwatana S, Khamanarong K, Chanthaooplee T. Shape of the lingula and its localization by panoramic radiograph versus dry mandibular measurement. *Surg Radiol Anat*. 2007; 29(8):689–694.
- Malamed SF. Techniques of mandibular anesthesia. In: *Handbook of Local Anesthesia*, 5th ed. St Louis: Mosby; 2004:228–35.
- Nicholson ML. A study of the mandibular foramen in the adult human mandible. *Anat Rec*. 1985; 212(1):110–2.
- Aggarwal V, Singla M, Kabi D. Comparative evaluation of anesthetic efficacy of Gow-Gates mandibular conduction anesthesia, Vazirani-Akinosi technique, buccal-plus-lingual infiltrations, and conventional inferior alveolar nerve anesthesia in patients with irreversible pulpitis. *Oral Surg Oral Med Oral Pathol Oral Radiol Endod*. 2010; 109(2):303–8.
- Goldberg S, Reader A, Drum M, et al. Comparison of the anesthetic efficacy of the conventional inferior alveolar, Gow-Gates and Vazirani-Akinosi techniques. *J Endod*. 2008; 34(11):1306–11.
- DeSantis JL, Liebow C. Four common mandibular nerve anomalies that lead to local anesthesia failures. *J Am Dent Assoc*. 1996; 127(7):1081–6.
- Oguz O, Bozkir MG. Evaluation of the location of the mandibular and mental foramina in dry, young, adult human male, dentulous mandibles. *West Indian Med J*. 2002; 51(1):14–6.
- Johnson TM, Badovinac R, Shaefer J. Teaching alternatives to the standard inferior alveolar nerve block in dental education: outcomes in clinical practice. *J Dent Educ*. 2007; 71(9):1145–52.
- Madan GA, Madan SG, Madan AD. Failure of inferior alveolar nerve block: exploring the alternatives. *J Am Dent Assoc*. 2002; 133(7):843–6.
- Archer WH. *Oral and maxillofacial surgery*, WB Saunders. 1975; 5(2): 1448–1449.
- Clark DE, Danforth RA, Barnes RW, Burtch ML. Radiation absorbed from dental implant radiography: a comparison of linear tomography, CT scan, and panoramic and intra-oral techniques. *J Oral Implantol*. 1990; 16(3):156–164.
- Mish CE. *Contemporary implant dentistry*, 3rd edn. Publisher: Elsevier Health Sciences; 2007:38–67.
- Kau CH, Richmond S, Palomo JM, Hans MG. Three-dimensional cone beam computerized tomography in orthodontics. *J Orthod*. 2005; 32(4):282–293.
- Joel Jaskari et al. Deep Learning Method for Mandibular Canal Segmentation in Dental Cone Beam Computed Tomography Volumes. *Scientific Reports* | (2020) 10:5842. <https://doi.org/10.1038/s41598-020-62321-3>.
- Lazzerini F, Minorati D, Nessi R, et al. The measurement parameters in dental radiography: a comparison between traditional and digital techniques. *Radiol Med*. 1996; 91(4):364–9.
- Ludlow JB, Laster WS, See M et al. Accuracy of measurements of mandibular anatomy in cone-beam computed tomography images. *Oral Surg Oral Med Oral Pathol Oral Radiol Endod*. 2007; 103(4):534–42.

23. Sonick M, Abrahams J, Faiella RA. A comparison of the accuracy of periapical, panoramic, and computerized tomographic radiographs in locating the mandibular canal. *J Oral Maxillofac Implants*. 1994; 9:455–60.
24. Pinsky HM, Dyda S, Pinsky RW, et al. Accuracy of three-dimensional measurements using cone-beam CT. *Dentomaxillofac Radiol*. 2006;35(6):410–6.
25. Altunsoy M, Ok E, Nur B, Gungor E, Colak M, Aglarci O. Localization of the mandibular foramen of 8-18 years old children and youths with cone-beam computed tomography. *J Pediatr Dent [Internet]*. 2014 ;2(2):44-48.
26. Russa AD, Fabian FM. Position of the mandibular foramen in adult male Tanzania mandibles. *Ital J Anat Embryol*. 2014;119(3):163–8.
27. Shayyab MH Al. A simple method to locate mandibular foramen with cone-beam computed tomography and its relevance to oral and maxillofacial surgery : a radio-anatomical study. *Surg Radiol Anat*.2018;40(6):625–34.
28. Daw JL Jr, Michael G, Aitken ME, Patel PK . The mandibular foramen: an anatomic study and its relevance to the sagittal ramus osteotomy. *J Craniofac Surg*. 1999; 10:475–479.
29. Park H-S, Lee J-H. A comparative study on the location of the mandibular foramen in CBCT of normal occlusion and skeletal class II and III malocclusion. *Maxillofac Plast Reconstr Surg [Internet]*. 2015;37(1):25.
30. Greenstein G, Cavallaro J, Tarnow D. Practical Application of Anatomy for the Dental Implant Surgeon. *J Periodontol [Internet]*. 2008;79(10):1833–46.
31. Devi R, Arna N, Manjunath KY. Incidence of morphological variants of mandibular lingula. *Indian J Dent Res*. 2003; 14:210–213.
32. Trost O, Salignon V, Cheyrel N, Malka G, Trouilloud P. A simple method to locate mandibular foramen: preliminary. Radiological study. *Surg Radiol Anat*. 2010; 32:927–931.
33. Reitzik M, Griffiths RR, Mirels H. Surgical anatomy of the ascending ramus of the mandible. *Br J Oral Surg*. 1976; 14:150–155.
34. Ennes JP, Medeiros RM, Grant JC. Localization of mandibular foramen and clinical implications. *Int J Morphol*. 2009; 27:1305–1311.
35. Kilarakaje N, Nayak SR, Narayan P, Prabhu LV. The location of the mandibular foramen maintains absolute bilateral symmetry in mandibles of different age groups. *Hong Kong Dent J*.2005; 2:35–37.
36. Kumar MP, Lokanadham S (2013) Sex determination and morphometric parameters of human mandible. *Int J Res Med Sci* 1:93–96.
37. Sairam V, Geethamalika MV, Kumar PB, Naresh G, Raju GP (2016) Determination of sexual dimorphism in humans by measurements of mandible on digital panoramic radiograph. *Contemp Clin Dent* 7:434–441.
38. Ashkenazi M, Taubman L, Gavish A. Age associated changes of the mandibular foramen position in anteroposterior dimension and of the mandibular angle in dry human mandibles. *Anat Rec*.2011; 294:1319–1325.
39. Kanno CM, de Oliveira JA, Cannon M, Carvalho AA. The mandibular lingula's position in children as a reference to inferior alveolar nerve block. *J Dent Child*. 2005; 72:56–60.
40. Tsai HH. Panoramic radiographic findings of the mandibular foramen from deciduous to early permanent dentition. *J Clin Pediatr Dent*. 2004; 28:215–219.